Impulsive Goodwin's Oscillator Model of Endocrine Regulation: Local Feedback Leads to Multistability

Zhanybai T. Zhusubaliyev, Alexander Medvedev, and Anton V. Proskurnikov

***Abstract*—The impulsive Goodwin's oscillator (IGO) is a hybrid model that captures complex dynamics arising in continuous systems controlled by pulse-modulated (event-based) feedback. Being conceived to describe pulsatile endocrine regulation, it has also found applications in e.g. pharmacokinetics. The original version of the IGO assumes the continuous part of the model to be a chain of first-order blocks. This paper explores the nonlinear phenomena arising due to the introduction of a local continuous feedback as suggested by the endocrine applications. The effects caused by a nonlinear feedback law parameterized by a Hill function are compared to those arising due to a simpler and previously treated case of affine feedback law. The hybrid dynamics of the IGO are reduced to a (discrete) Poincaré map governing the propagation of the model's continuous states through the firing instants of the impulsive feedback. Bifurcation analysis of the map reveals in particular that both the local Hill function and affine feedback can lead to multistability, which phenomenon has not been observed in the usual IGO model.**

I. INTRODUCTION

Impulsive mathematical models [1] are instrumental in describing systems that comprise subsystems with relatively fast dynamics interacting with subsystems possessing slow dynamics. Then the fast dynamics components can be reduced to impulse trains impacting the components with slow dynamics. In general, the timing and the amplitudes of the impulses are modulated by variables that belong to the slow dynamics part of the system thus giving rise to a hybrid (i.e. continuous-discrete) model of the system [2], which can often be considered as a feedback loop comprising a continuous-time plant and a discontinuous event-triggered feedback law that portrays a biological (endogenous or exogenous) pulsatile controller.

In biological systems, the slow and fast dynamical parts often have different underlying nature. Electrical neural signaling that regulates continuous biochemical subsystems is ubiquitous in endocrinology [3] and metabolism [4]. Episodic impacts can also be mediated biomechanically by contracting and relaxing muscles that affect a liquid flow [5]. Naturally, the muscles are neurally controlled and, in this case, act as actuators.

Zh. T. Zhusubaliyev is with the Department of Computer Science, Dynamics of Non-Smooth Systems International Scientific Laboratory, Southwest State University, 50 Years of October Str. 94, 305040, Kursk, Russia zhanybai@hotmail.com

A. Medvedev is with the Department of Information Technology, Uppsala University, SE-752 37 Uppsala, Sweden alexander.medvedev@it.uu.se

Anton V. Proskurnikov is with Department of Electronics and Telecommunications, Politecnico di Torino, Turin, Italy, and Institute for Problems of Mechanical Engineering of the Russian Academy of Sciences , St. Petersburg, Russia, anton.p.1982@ieee.org

This work was supported by the Ministry of Science and Higher Education of the Russian Federation (Project No. 075-15-2021-573).

A. Pulsatile endocrine regulation

The endocrine system of an organism is constituted by glands communicating through hormone molecules as messengers [6]. Hormones are chemical blood-borne substances produced by the glands and regulate biological vital functions such as metabolism, reproduction, and growth. The endocrine system is an example of a complex dynamical network with multiple positive (stimulatory) and negative (inhibitory) couplings between the nodes that correspond to individual glands. The endocrine system is orchestrated by the dedicated neural centers of the brain, primarily, the *hypothalamus* and the *pituitary gland* (hypophysis). The former produces concentration pulses of so-called release hormones (releasing factors) that communicate control information to the glands through pulse amplitude and frequency, see e.g. [7]. The neuroendocrine control loop incorporating the hypothalamus and the involved endocrine glands is thus an example of *impulsive* (pulse-modulated) control system [1].

Mathematically tractable models are usually obtained by decoupling the endocrine system into smaller subsystems, called hormonal *axes*, capturing only essential characteristics and interactions [8]. In spite of different biological characteristics of the hormones (secretion and clearance rates, temporal patterns of concentration evolution, etc.), structures of endocrine axes regulating testosterone, cortisol, growth, adrenal and parathyroid hormones are similar [3], [9], [10].

The structural diagram of a neuroendocrine axis is shown in Fig. 1 and possesses two negative feedback loops. The outer ("long") feedback implements impulsive event-triggered control through impulses of a so-called release hormone from the hypothalamus, whose amplitude and frequency are modulated by the concentration of the effector hormone in the bloodstream. It is generally hypothesized that the purpose of the impulsive regulation loop is to maintain timed rhythmic activity in the concentrations of the involved hormones with minimal means. The inner (or *local*) feedback from the target gland to the pituitary is enabled by the presence of effector hormone receptors in the pituitary but its strength apparently differs between species [11]. The inner feedback is therefore continuous in nature. As reported in [9], the third negative feedback from the pituitary gland to the hypothalamus also exists, but its effect is much weaker than the effects of two feedback loops, so its usually neglected to reduce model complexity.

B. Goodwin's oscillator

The classical Goodwin's oscillator (GO) [13], [14] serves as a basis for many biochemical models and constitutes a

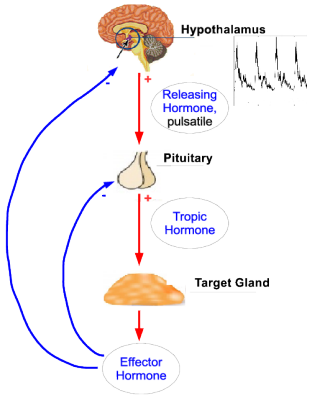

Fig. 1. A scheme of hypothalamus-pituitary endocrine axis [12]

prototypical biological oscillator. At the same time, its original version has numerous limitations [12], [15]–[17] and fails to capture many important features of the actual biological mechanism; In particular, the classical GO is continuous, whereas the dynamics of endocrine axes are hybrid due to the presence of impulsive phenomena.

The current extensions of the GO can be divided into two groups. Models of the first type [18]–[25] modify the structure of the original GO and consider more complex interactions between the model states that obey nonlinear ordinary or delay-differential equations. Their dynamics, however, remain continuous, which allows to use well-developed techniques of ordinary differential equations, ranging from local stability analysis and Hopf bifurcations to recent extensions of Poincaré-Bendixson theorems [26].

In many biomedical applications, biochemical processes are controlled by neural populations and centers through impulsive feedback action contributed by firing neurons. This class of systems gives rise to the models of the second kind [27]–[32]. Being historically focused on the testosterone regulation in the male, they preserve the original structure of the GO and yet portray the *pulsatile* mechanism of secreting the release hormone, which phenomenon is established by numerous experimental studies [8], [33], [34]. To cope with the hybrid (impulsive and continuous) dynamics of such models, special techniques from theory of impulsive systems [1] have been utilized. Unlike the classical continuous GO, the hybrid model in [28] (i.e. the IGO) has no equilibria by design and is proved to possess periodic trajectories. In particular, a unique solution with one pulse over the period (1-cycle) exists [28]; periodic solutions with $m \geq 2$ pulses per period (m-cycles) may also exist [32]. A hybrid model with equilibrium can be obtained from the IGO by allowing for impulses of zero weight [5]. This special case is motivated by the necessity of modeling transient oscillations, e.g. in the blood concentration of a drug after single-dose administration.

Although the rich dynamics of IGO can approximate measured hormone concentration profiles quite well [28], this model ignores the local feedback from the target gland to the pituitary and, thus, does not reflect the full structure of the hormone interactions in Fig. 1. In order to study the effect of this local feedback, an extension termed the impulsive Goodwin's oscillator with a local feedback (IGOLF) has been introduced in [12]. The local feedback can be reasonably assumed to be continuous, as the corresponding loop does not involve the hypothalamus. As discussed in [12], there is no consensus on the mathematical description of the respective feedback control mechanism. From a system identification perspective [35]–[37], it is desirable to consider models that *linearly* depend on unknown parameters rather than identify the nonlinear functions that usually arise in the kinetic equations [14].

Beyond the saturation intervals corresponding to extreme values of the regulated variable, a Hill-function nonlinearity can be well approximated by an affine function, as proposed in [12], where the IGOLF model with an *affine* negative feedback is considered. It has been shown that, for a low-gain local feedback of this type, the IGOLF model inherits many properties of IGO [28] and, moreover, can be reduced to the IGO by an affine transformation. The price paid for the affine structure of local feedback is, however, the occurrence of partially negative trajectories. Although negative concentration values of a substance in the bloodstream allow a plausible biological interpretation (the substance deficit in homeostasis), their occurrence undermines the model cogency. At the same time, with a proper choice of the parameters, the IGOLF model exhibits *periodic* solutions that are positive and hence biologically feasible. Notably, the latter property applies only to the case of an affine local feedback but, in general, fails to hold for a linear feedback.

Although the feedback approximation by an affine function simplifies somehow the analysis of the IGOLF model, more sophisticated choices (in particular, the Hill function) are typically made in biological models. A clear disadvantage of affine negative feedback is the existence of biologically infeasible solutions. The use of positive Hill-function nonlinearities automatically ensures feasibility of the solutions, adding however to the diversity in the model's dynamical behaviors.

The present paper demonstrates that the introduction of a local Hill-function feedback in the IGO leads to the appearance of e.g. multistability (that is, coexistence of several stable attractors) as well as crises of chaotic attractors. In order to understand the mechanism leading to these phenomena, a comparison between IGOLF models with a nonlinear Hill-type function and with its affine approximation is preformed. We explain also which features of the behavior of the nonlinear feedback model are captured by the affine feedback model and which are not. It should be noted that the model with affine feedback, arising as an approximation of the Hill function, does not satisfy the "small gain" condition from [12], and thus is not reducible to the IGO model previously studied in [28]. In fact, the IGOLF model that is studied in this paper acquires new properties that are not exhibited by the original IGO model without local feedback. To examine the IGOLF numerically, its hybrid dynamics are reduced to a discrete-time system, or the Poincaré map, governing the propagation

of the model's continuous states through the firing instants of the impulsive feedback.

The paper is organized as follows. In Section II, we briefly review the Goodwin-type models used in modeling of hormonal axes, introducing, in particular, the IGO and IGOLF models. In Section III, bifurcation analysis of the simpler model with an affine local feedback is carried out. Section IV deals with a more complicated nonlinear model. Section V concludes the paper.

II. PRELIMINARIES: GOODWIN-TYPE MODELS

This section briefly reviews the GO and introduces its extensions to be studied in the rest of the paper.

A. The classical Goodwin's oscillator

The *classical* continuous GO [13] involves three variables x_1, x_2, x_3 that in our case stand for serum concentrations of the release, tropic, and effector hormones, respectively. The variables obey the equations

$$\begin{aligned} \dot{x}_1 &= -b_1 x_1 + f(x_3), \\ \dot{x}_2 &= -b_2 x_2 + g_1 x_1, \\ \dot{x}_3 &= -b_3 x_3 + g_2 x_2. \end{aligned} \tag{1}$$

Here $b_i, g_i > 0$ and the function $f : [0,\infty) \to [0,\infty)$ describe the production and clearing rates of the hormones; $f(\cdot)$ is decreasing (thus $f(0) > 0$) and represents the negative (inhibitory) coupling from the last to the first hormone in the chain, see Fig. 1. The decrease in the level of effector hormone stimulates the production of the release hormone, which in turn stimulates of the effector hormone (through the additional tropic hormone). The nonlinear feedback is typically characterized by the *Hill* function [15]

$$f(x_3) = \frac{a}{1 + b(x_3/h)^m}, \quad a, b, h > 0, m \geq 1. \tag{2}$$

The properties of GO (1), (2) are surveyed in [14], [15], [17], [25] and references therein. It is known that the model has a unique equilibrium in the positive octant $x_1, x_2, x_3 > 0$. This equilibrium can be unstable only when the Hill constant $m > 8$, otherwise, the model has a locally stable equilibrium. Simulations indicate that, in fact, all positive trajectories converge to the equilibrium, which fact has still to be proved mathematically. If the equilibrium is unstable, then almost all trajectories converge to periodic orbits [25].

B. The impulsive Goodwin's oscillator (IGO)

The key limitation of the classical GO is its incoherence with the actual discontinuous mechanism of the release hormone secretion in the hypothalamus. The jumps in the hormone concentration x_1 observed in experiments [28], [38] can be modeled by replacing the continuous function $f(x_3)$ in (1) with a pulse-modulated feedback mechanism [28]. Equations (1) are thus substituted by

$$\begin{aligned} \dot{x}_1 &= -b_1 x_1, \\ \dot{x}_2 &= -b_2 x_2 + g_1 x_1, \quad t \in (t_k, t_{k+1}), \\ \dot{x}_3 &= -b_3 x_3 + g_2 x_2, \end{aligned} \tag{3}$$

$$x_1(t_k^+) = x_1(t_k^-) + \lambda_k,\ x_2(t_k^+) = x_2(t_k^-),\ x_3(t_k^+) = x_3(t_k^-). \tag{4}$$

The instantaneous jumps in x_1 given by (4) correspond to onset of release hormone pulses. The pulses are produced by a pulse-modulation mechanism implementing the "long" feedback from the effector to the release hormone (Fig. 1). The sequences of the pulse instants t_k and amplitudes λ_k depend on a specific solution to model (3), (4). An important assumption, based on experimental evidence [39], is that, in this feedback mechanism, the amplitude λ_k and the inter-pulse interval $(t_{k+1} - t_k)$ depend only on the state of the system at time t_k, but not on the previous trajectory:

$$\lambda_k = F(x_3(t_k)), \quad t_{k+1} = t_k + \Phi(x_3(t_k)), \quad t_0 = 0, \tag{5}$$

where the functions Φ, F are strictly positive and bounded

$$\begin{aligned} &\Phi : \mathbb{R} \to [\Phi_1, \Phi_2], \qquad F : \mathbb{R} \to [F_1, F_2], \\ &0 < \Phi_1 < \Phi_2 < \infty, \quad 0 < F_1 < F_2 < \infty. \end{aligned} \tag{6}$$

Such a feedback mechanism is referred to as a pulse amplitude-frequency modulator of the first kind [1] or an impulsive self-triggered controller [40]. The assumption $t_0 = 0$ does not result in loss of generality and means that the system operation starts with the first pulse.

In (6), the amplitude modulation characteristic F is *non-increasing*, while the frequency modulation characteristic Φ is assumed to be *non-decreasing*. This agrees with the experimental observations reported in e.g. [38]. An increase of the effector hormone level decreases the frequency of release hormone pulses and reduces their amplitudes [38], thus also suppressing the bursts of the intermediate tropic hormone.

The properties of system (3)-(5) constituting the IGO are well documented in [28]–[32]. The most important difference from the classical GO is the existence of periodic solutions and absence of fixed points due to the persistent pulses. Moreover, a periodic solution with a single jump over the least period (1-cycle) always exists and is unique [28].

C. From IGO to IGOLF: Additional feedback

Whereas the pulsatile mechanism of the "long" feedback in Fig. 1 is captured by the IGO model (3)-(5), this model ignores the existence of a *local* feedback. A natural question arises whether such a local feedback changes the model properties and leads to new dynamical phenomena.

An important step in the analysis of IGO with additional local feedback (IGOLF) was taken in [12]. The local feedback can be reasonably assumed to be continuous, as it does not involve impulsive mechanisms of hypothalamus; On the other hand, there is no consensus on the form of this nonlinearity. The local feedback typically cannot be experimentally observed in its full domain of definition [37]. Beyond the

saturation intervals of extreme hormone concentration, the Hill function and other nonlinearities can be well approximated by polynomials. It was proposed to approximate the "local" feedback by the simplest first-order polynomial, or the *affine function* $\mu - k_d x_3$, where $\mu, k_d \geq 0$ are some coefficients. The continuous part of the IGO model in (3) is then replaced by

$$\begin{aligned} \dot{x}_1 &= -b_1 x_1, \\ \dot{x}_2 &= -b_2 x_2 + g_1 x_1 - k_d x_3 + \mu, \\ \dot{x}_3 &= -b_3 x_3 + g_2 x_2, \quad t \in (t_n, t_{n+1}), \end{aligned} \tag{7}$$

whereas equations (4) and (6) remain unchanged.

The constant $k \geq 0$ in (7) stands for the *control gain*, regulating the dependence between the level of the effector hormone and the secretion of the tropic hormone in the pituitary gland. The constant μ may be interpreted as the hormone's basal level, i.e. the product of the hormone secretion outside the feedback loop. Note here that removing μ simplifies the model, but then the system may have no positive solutions for some parameters b_i, g_i.

The main mathematical result from [12] is concerned with the case of k_d being sufficiently small, so that the characteristic polynomial of the linear part

$$\chi(\lambda) = (\lambda + b_1)[(\lambda + b_2)(\lambda + b_3) + g_2 k_d] \tag{8}$$

has only *real* zeros. This holds if and only if

$$0 \leq k_d < k_* := \frac{(b_2 - b_3)^2}{4 g_2}.$$

Under this assumption, the IGOLF given by (7), (4), (6) reduces, in fact, to the IGO in (3)-(6) through a linear transformation of variables. The inverse transformation can however map a positive (biologically feasible) solution into a partially negative solution. Nevertheless, choosing $\mu > 0$ large enough, it can be guaranteed that all periodic solutions of the system are positive.

In what follows, we consider a more complicated situation, when the polynomial $\chi(\lambda)$ has only one real root and a pair of complex-conjugate roots. Then, the dynamics of (7), (4), (6) become much more complicated and cannot be reduced to the IGO model. By using numerical analysis, we in fact show that the IGOLF in this situation obtains new properties that do not appear in the IGO model, e.g. multistability.

Furthermore, we compare the behaviors of this model and the more complicated model with Hill-function local feedback, whose continuous part is described by the equation

$$\begin{aligned} \dot{x}_1 &= -b_1 x_1, \\ \dot{x}_2 &= -b_2 x_2 + g_1 x_1 + \frac{a}{1 + \kappa \cdot (x_3/r)^s}, \\ \dot{x}_3 &= -b_3 x_3 + g_2 x_2, \quad t \in (t_n, t_{n+1}), \end{aligned} \tag{9}$$

Here $a, \kappa, r > 0$ and $s \geq 1$ are constant parameters.

III. IGOLF With Affine Local Feedback

We first consider system (7), (4), (5) whose structure is simpler than the structure of IGOLF with Hill-function feedback and whose dynamics essentially reduces to a *discrete mapping*, for which a closed-form expression is available.

Below, we assume that characteristic polynomial (8) (which is Hurwitz[1] when $b_1, b_2, b_3, g_2 > 0$ and $k_d \geq 0$) has only one real root $\lambda_1 = -b_1$ and a pair of complex-conjugate roots $\lambda_{2,3} = \alpha \pm \beta \mathbf{i}$, where

$$\alpha = -\frac{b_2 + b_3}{2} < 0, \quad \beta = \sqrt{b_2 b_3 + g_2 k_d - \frac{(b_2 + b_3)^2}{4}} > 0.$$

In the present case, the algebraic transformation reducing the IGOLF to the IGO from [12] is undefined. As presented in the next subsections, bifurcation analysis reveals a deep geometric reason for this: the dynamics of the IGOLF in the case of complex eigenvalues are much richer than dynamics of the IGO and are featured by multistability, in particular, chaotic attractors may coexist with stable cycles.

Following [28], we assume that the modulation functions in (6) are given by

$$\Phi(x_3) = k_1 + k_2 \frac{(x_3/h)^p}{1 + (x_3/h)^p}, \; F(x_3) = k_3 + \frac{k_4}{1 + (x_3/h)^p}. \tag{10}$$

A. Discrete-time map

To facilitate the analysis, introduce the new variables $\bar{x}$, $\bar{y}$ and $\bar{z}$ that are related to x_1, x_2, x_3 as follows

$$\begin{aligned} x_1 &= [(b_1 + \alpha)^2 + \beta^2] \cdot \bar{x}, \\ x_2 &= -g_1(b_1 + b_2 + 2\alpha) \cdot \bar{x} - g_1(b_2 + \alpha) \cdot \bar{y} \\ &\quad - g_1 \beta \cdot \bar{z} + \frac{b_3 \mu}{b_2 b_3 + g_2 k_d}, \\ x_3 &= g_1 g_2 (\bar{x} + \bar{y}) + \frac{g_2 \mu}{b_2 b_3 + g_2 k_d}. \end{aligned} \tag{11}$$

Substituting (11) into (7) and solving with respect to the derivatives, we obtain

$$\frac{d\bar{x}}{dt} = \lambda_1 \bar{x}, \quad \frac{d\bar{y}}{dt} = \alpha \bar{y} - \beta \bar{z}, \quad \frac{d\bar{z}}{dt} = \beta \bar{y} + \alpha \bar{z}, \tag{12}$$

whereas equations (4),(6) transform into

$$\begin{gathered} \bar{x}(t_k^+) = \bar{x}(t_k^-) + \gamma_0 F(\varphi(t_k)), \quad \bar{y}(t_k^+) = \bar{y}(t_k^-) - \gamma_0 F(\varphi(t_k)), \\ \bar{z}(t_k^+) = \bar{z}(t_k^-) - \gamma_1 F(\varphi(t_k)), \quad t_{k+1} = t_k + \Phi(\varphi(t_k)). \end{gathered}$$

In the equations above, we have

$$\begin{gathered} \varphi(t) = g_1 g_2 (\bar{x}(t) + \bar{y}(t)) + \frac{g_2 \mu}{b_2 b_3 + g_2 k_d} = x_3(t), \\ \gamma_0 = \frac{1}{(b_1 + \alpha)^2 + \beta^2} \quad \text{and} \quad \gamma_1 = \frac{b_1 + \alpha}{\beta} \gamma_0. \end{gathered}$$

It can be easily seen that the whole trajectory of the system is uniquely recovered from the behavior of the discrete-time sequence $\{(\bar{x}_k, \bar{y}_k, \bar{z}_k)\}$, defined as

$$\bar{x}_k = \bar{x}(t_k^-), \bar{y}_k = \bar{y}(t_k^-), \bar{z}_k = z(t_k^-).$$

The values $\bar{x}(t), \bar{y}(t), \bar{z}(t)$ for $t \in (t_k, t_{k+1})$ are found by direct integration of linear equations (12).

[1]Recall that a polynomial is Hurwitz if all its roots have negative real parts.

For this reason, analysis of the nonlinear IGOLF model reduces to the analysis of *discrete-time* dynamics, which can be expressed explicitly

$$\begin{aligned}
\bar{x}_{k+1} &= \mathrm{e}^{\lambda_1 T_k}\cdot(\bar{x}_k+\Gamma_k);\\
\bar{y}_{k+1} &= \mathrm{e}^{\alpha T_k}\cdot[(\bar{y}_k-\Gamma_k)\cdot\cos(\beta T_k)-(\bar{z}_k-\Omega_k)\cdot\sin(\beta T_k)];\\
\bar{z}_{k+1} &= \mathrm{e}^{\alpha T_k}\cdot[(\bar{y}_k-\Gamma_k)\cdot\sin(\beta T_k)+(\bar{z}_k-\Omega_k)\cdot\cos(\beta T_k)],
\end{aligned} \tag{13}$$

and here T_k,Γ_k,Ω_k are functions of $\bar{x}_k,\bar{y}_k$ defined by

$$\begin{aligned}
T_k=\Phi(\varphi_k),\quad \Gamma_k=\gamma_0 F(\varphi_k),\quad \Omega_k=\gamma_1 F(\varphi_k),\\
\varphi_k = g_1 g_2(\bar{x}_k+\bar{y}_k)+\frac{g_2\mu}{b_2b_3+g_2k_d},\\
\gamma_0=\frac{1}{(b_1+\alpha)^2+\beta^2}\quad\text{and}\quad \gamma_1=\frac{b_1+\alpha}{\beta}\,\gamma_0.
\end{aligned} \tag{14}$$

Substituting (14) into the right-hand side of (13), one finds the *discrete map*

$$\mathfrak{M}:(\bar{x}_k,\bar{y}_k,\bar{z}_k)\mapsto(\bar{x}_{k+1},\bar{y}_{k+1},\bar{z}_{k+1}).$$

B. Cycles

Dealing with hormonal rhythms, we are primarily interested in *periodic* solutions of the model. It can be shown that periodic trajectories lead to periodic sequences $(\bar{x}_k,\bar{y}_k,\bar{z}_k)$, and vice versa. Therefore, if the discrete-time dynamics are periodic, the continuous solution is periodic, too. Notice that the time elapsed between the subsequent jumps $t_{k+1}-t_k$ is *strictly positive* by construction. Given the solution least period T, each interval $[t,t+T)$ contains only a finite number of jumping instants. Such periodic solution is called an *m-cycle*, where $m\geq 1$ and, obviously, does not depend on t.

Evidently, 1-cycles stand for the *fixed points* of the discrete map $\mathfrak{M}$. More generally, m-cycles correspond to the points of period m, that is, such point $r=(\bar{x},\bar{y},\bar{z})$ that

$$m=\min\{k\geq 1:\mathfrak{M}^k(r)=r\}.$$

C. Bifurcation analysis

In [12], it was illustrated both analytically and numerically that the presence of an affine negative feedback compromises solution positivity. By choosing μ large enough, one can guarantee positivity of all periodic solutions. However, on the other hand, the local feedback may lead to more complicated dynamical behaviors, such as multistability (coexistence of several stable attractors) and hysteresis transitions [41], [42].

The purpose of this section is to illustrate some mechanisms involved in the appearance of the multistability. For the simulation, we use the following parameters: $b_2=0.1$, $b_3=0.06$, $k_1=42.0$, $k_2=82.0$, $k_3=0.05$, $k_4=5.0$, $h=2.7$, $p=4$. Remaining parameters b_1, g_1, g_2, $k_d=0.042$ and $\mu=0.07$ are varied.

Fig 2(a) displays the coexistence of the two stable cycles and hysteretic transitions from the one stable motion to another and vice versa. The bifurcation diagrams in Fig 2(a) obtained through direct simulation also show a period doubling transition to chaos. To better illustrate hysteretic transitions, a magnified part of Fig. 2(a) is presented in Fig. 2(b). This diagram is obtained by following the stable and saddle 4-cycles.

As the parameter b_1 decreases/increases, the stable 4-cycle O_1/O_2 merges with the saddle 4-cycle O_3 and disappears in a fold (saddle-node) bifurcation (Fig. 2(b)). The domain between the fold bifurcation points $b_1^{1,\text{fold}}$ and $b_1^{2,\text{fold}}$ are the region of bistability where the two stable 4-cycles coexist. When crossing the boundaries $b_1^{1,\text{fold}}$ and $b_1^{2,\text{fold}}$ of the bistability region, the system displays hysteretic transitions from the one stable 4-cycle to another and vice versa. Fig. 2(c) illustrates a form of multistability when the stable periodic motions, arising in a fold bifurcation, can undergo a classical infinite sequence of period-doubling bifurcation, leading to the transition to chaos, see Fig. 2 (a),(c). As a result, we have parameter domains where a chaotic attractor coexists alongside with stable cycles, Fig. 2(c).

Note that the ordinate axis x_3 in Fig. 2 is the third dynamical variable of (7) interpreted as the concentration of effector hormone (testosterone, cortisol, growth hormone etc.), which is related to the dimensionless variables of (12) through linear transformation (11). Next, we will stick to the same notation.

A distinctive feature of multistable systems is their sensitivity to dsiturbance: an arbitrarily small level of perturbation may cause a sudden transition from one attractor to another, i.e. a fundamentally unpredictable behavior of the system. A broad discussion of the role of the multistability in complex dynamics can found for instance in a series of publications by Feudel et al. [41], [42].

IV. IGOLF With Hill-function Local Feedback

Although the IGOLF model with affine feedback has a number of disadvantages (such as e.g. the existence of biologically infeasible negative solutions) and is limited in its ability to describe actual biochemical feedback mechanisms, our studies of this model reveal actually the *same* phenomena (e.g. multistability, crises of the chaotic attractors etc.) as those observed in the more complicated IGOLF model with Hill-function local feedback (9),(4),(5). Similar to the previous case, we choose the pulse modulator characteristics in the form of (10). Note that if $a=0$, then continuous block (9) reduces to (3), and the model degenerates to the IGO from [28].

In the numerical simulations, the following parameters were used: $0.13<b_1<0.14$, $b_2=0.1$, $b_3=0.06$, $g_1=0.8$, $g_2=0.18$, $k_1=42.0$, $k_2=82.0$, $k_3=0.05$, $k_4=5.0$, $h=2.7$, $p=3$, $r=1.2$, $a=4.5$, $\kappa=1.0$ and $s=3$.

Fig. 3(a) provides an overview of the formation of coexisting modes, appearance of chaos via a cascade of period-doubling bifurcations, and transitions from a small-size to a large-size chaotic attractor in an expansion bifurcation.

Inspection of this diagram shows that stable 4-cycle O_3 that is arising in a fold bifurcation at $b_1^{3,\text{fold}}$ coexists with a stable fixed point O_4. As the parameter b_1 decreases, one can observe an infinite sequence of period-doubling bifurcation, leading to the transition to chaos. This type of transition also is observed when the parameter b_1 increases from the value

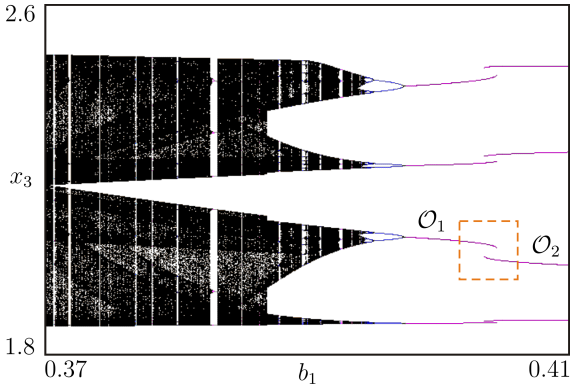

(a)

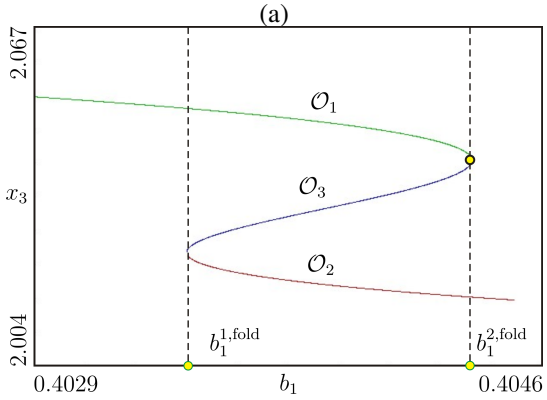

(b)

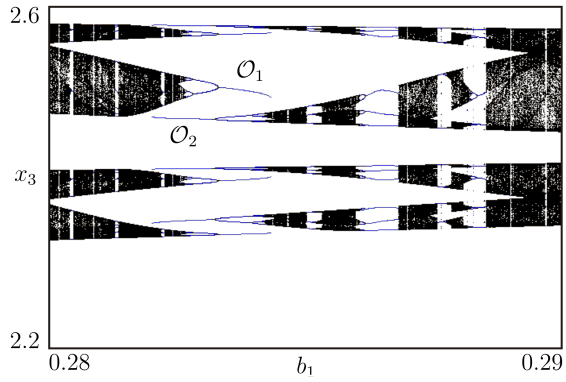

(c)

Fig. 2. (a) Bifurcation diagram showing the coexistence of two stable 4-cycles (O_1, O_2) and a period doubling transition to chaos, $0.37 < b_1 < 0.41$, $k_d = 0.028$ and $\mu = 0.062$. (b) Magnified part of the bifurcation diagram that is outlined by the red rectangle in (a) illustrating hysteretic transition from one stable 4-cycle O_1 to another O_2 and vice versa in a fold (saddle-node) bifurcation. $b_1^{1,\text{fold}}$ and $b_1^{2,\text{fold}}$ are the fold bifurcation points. The stable manifold of a saddle 4-cycle O_3 delineates the basins of attraction for coexisting stable cycles O_1 and O_2. (c) Bifurcation diagram illustrating the coexistence of periodic and chaotic attractors, $0.28 < b_1 < 0.29$, $k_d = 0.0268$ and $\mu = 0.06208$.

$b_1^{1,\text{fold}}$, at which the stable O_1 and saddle O_2 4-cycles appear in a fold bifurcation.

It should be noted that at the points $b_1^{1,\text{h}}$ and $b_1^{2,\text{h}}$, the chaotic attractors, which occur through a period-doubling cascade, suddenly increase in size. Such type of transition is known as an expansion bifurcation [43] or an interior crisis [44], [45].

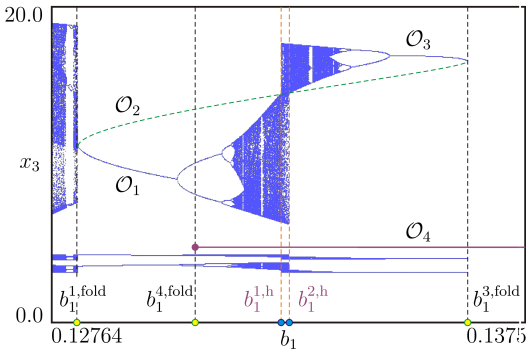

(a)

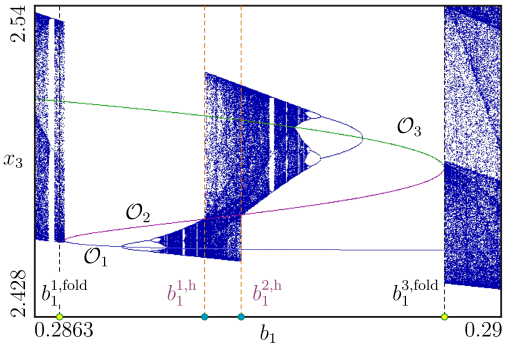

(b)

Fig. 3. (a) Bifurcation diagram for (9). The diagram illustrates a form of multistability in which stable fixed point O_4 and periodic or chaotic attractor coexist. Here $b_1^{1,\text{fold}}$, $b_1^{3,\text{fold}}$, are the fold bifurcation points at which the stable O_1 and saddle O_2 cycles or stable O_3 and saddle O_2 points are born, respectively. $b_1^{4,\text{fold}}$ is the saddle-node bifurcation point for the fixed point O_4. $b_1^{1,\text{h}}$ and $b_1^{2,\text{h}}$ denote the expansion bifurcation point at which a chaotic attractor suddenly increases in size. (b) Bifurcation diagram for the affine model illustrating an expansion bifurcation, that is shown in (a).

Consider the characteristics of this bifurcational behavior in more detail in order to understand the mechanism of the transition. Expansion bifurcation is associated with homoclinic bifurcations and it is very difficult to study in detail using a model with a Hill-function feedback. In this case, the role of the affine model is very important.

Fig. 3(b) shows the bifurcation diagram for the affine feedback model obtained by means of continuation techniques. This diagram illustrates the expansion bifurcation, that is shown in Fig. 3(a). This transition is caused by the contact of the chaotic attractor with the stable manifold of the saddle cycle O_2 (see Fig. 3(a),(b)), or, in other words, by the homoclinic tangency between the stable and the unstable manifolds of the O_2 [46]. As a result, the chaotic attractor merges with the chaotic repeller. This leads to an abruptly changing amplitude of the chaotic oscillations. The domain between the points $b_1^{1,\text{h}}$ and $b_1^{2,\text{h}}$ is a region where the large-size chaotic attractor coexists with the stable fixed point O_4. When crossing the boundaries $b_1^{1,\text{h}}$ and $b_1^{2,\text{h}}$ the system displays expansion bifurcations.

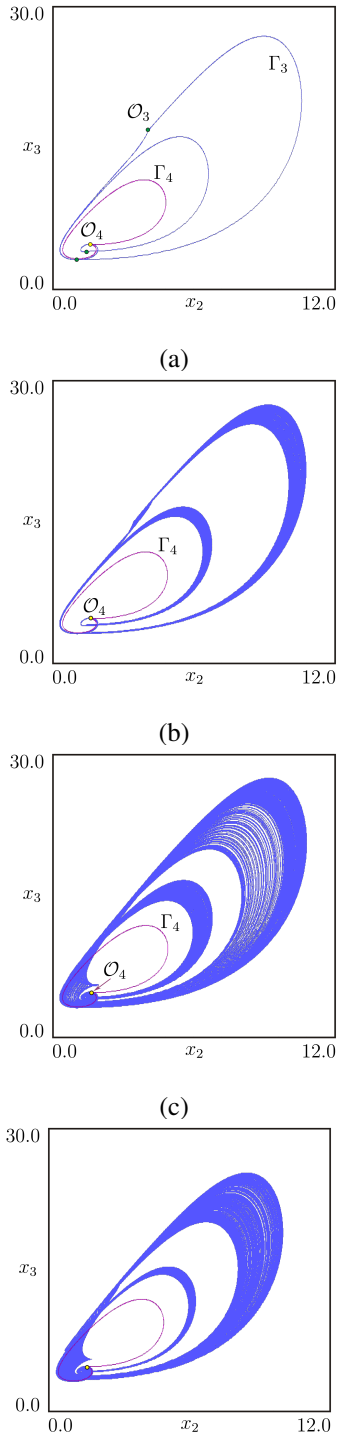

Fig. 4. (a) Coexistence of a stable 3-cycle O_3 and a stable fixed point O_4 for $b_1 = 0.1348$ in Fig. 2(a). (b) Phase portrait for $b_1 = 0.132893334$ near the expansion bifurcation point $b_1^{2,\mathrm{h}}$ where a stable fixed point O_4 coexists with a small-size chaotic attractor. (c) Phase portrait for $b_1 = 0.13249384646$ in the region between the expansion bifurcation points $b_1^{1,\mathrm{h}}$ and $b_1^{2,\mathrm{h}}$. (d) Phase portrait for $b_1 = 0.1317$ that falls to the left of the point $b_1^{2,\mathrm{h}}$.

Fig. 4(a) shows the phase portrait of (9) for the values of b_1 where the stable 4-cycle O_3 coexists with a stable fixed point O_4. The phase portrait contains the periodic orbits Γ_4 and Γ_3 of the Eq. (9), and corresponding fixed O_4 and periodic O_3 points of the map for a vector field (9). Fig. 4(b) displays the phase portrait near the first expansion bifurcation (for the value of b_1 that falls to the right of the point $b_1^{2,\mathrm{h}}$). At this stage, the stable fixed point O_4 coexists with a small-size chaotic attractor.

Fig. 4(c) shows the phase portrait after the first expansion bifurcation as b_1 decreases from the value $b_1^{3,\mathrm{fold}}$. The boundary of this bifurcation is denoted as $b_1^{2,\mathrm{h}}$. Here, the stable fixed point O_4 coexists with a large-size chaotic attractor. With further decrease of b_1, the second expansion bifurcation occurs at $b_1^{1,\mathrm{h}}$ when the stable and unstable manifolds of the period-4 saddle cycle become tangent to each other (the second homoclinic tangency). After the homoclinic tangency, the chaotic attractor suddenly changes in size. Fig. 4(d) shows the phase portrait after the second expansion bifurcation. Comparing Fig. 4(b) and Fig. 4(d), one can conclude that in region between the points $b_1^{1,\mathrm{h}}$ and $b_1^{2,\mathrm{h}}$ the stable and unstable manifolds of the period-4 saddle cycle intersect transversally to form a homoclinic structure. The intersection of these manifolds implies, that the two small-size chaotic attractors (in Figs 4(b) and 4(d)) "merge" into a single large-size one (Fig 4(c)).

V. Conclusion

The present work deals with the dynamic features of an impulsive Goodwin's oscillator [27], [28] that was modified in [12] by introducing a local nonlinear continuous feedback. We have demonstrated that this addition resulted in new complex dynamical behaviors such as multistability and crises of chaotic attractors. In order to understand the mechanisms behind these phenomena, we apply a modeling approach based on the approximation of a nonlinear continuous feedback by an affine feedback. Due to its simplicity, this model allowed us to perform a detailed numerical bifurcation analysis. The affine model is of course strongly limited in its ability to account for the many complicated mechanisms taking place in the model with a Hill-function feedback. In particular, the presence of an affine negative feedback gives rise to the problem of solution positivity. However, it still can be useful in the analysis of global dynamics that are associated with homoclinic bifurcations, showing similar properties to those of the Hill-function feedback model.

One topic of ongoing research is to find a procedure for identification of the IGOLF model's parameters, which will allow, in particular, to compare the model's predictions with experimental data provided in [28].

References

[1] A. K. Gelig and A. N. Churilov, *Stability and Oscillations of Nonlinear Pulse-modulated Systems*. Boston: Birkhäuser, 1998.

[2] R. Goebel, R. G. Sanfelice, and A. R. Teel, *Hybrid Dynamical Systems. Modeling, Stability, and Robustness*. Princeton University Press, 2012.

[3] W. S. Evans, L. S. Farhy, and M. L. Johnson, "Biomathematical modeling of pulsatile hormone secretion: a historical perspective," in *Methods in Enzymology: Computer methods, Volume A*, M. L. Johnson and L. Brand, Eds., 2009, vol. 454, pp. 345–366.

[4] A. Niijima, "Nervous regulation of metabolism," *Progress in Neurobiology*, vol. 33, no. 2, pp. 135–147, 1989.

[5] H. Runvik, A. Medvedev, and M. C. Kjellsson, "Impulsive feedback modeling of levodopa pharmacokinetics subject to intermittently interrupted gastric emptying," in *American Control Conference*, Denver, CO, 2020.

[6] K. L. Becker, J. P. Bilezikian, W. J. Bremner, and W. Hung, *Principles and Practice of Endocrinology and Metabolism*, 3rd ed. Lippincott Williams & Wilkins, 2001.

[7] J. J. Walker, J. R. Terry, K. Tsaneva-Atanasova, S. P. Armstrong, C. A. McArdle, and S. L. Lightman, "Encoding and decoding mechanisms of pulsatile hormone secretion," *J. Neuroendocrinoly*, vol. 22, no. 12, pp. 1226–1238, 2009.

[8] D. M. Keenan and J. D. Veldhuis, "A biomathematical model of time-delayed feedback in the human male hypothalamic-pituitary-Leydig cell axis," *Amer. J. Physiology. Endocrinology and Metabolism*, vol. 275, no. 1, pp. E157–E176, 1998.

[9] E. B. Stear, "Application of control theory to endocrine regulation and control," *Annals of biomedical engineering*, vol. 3, no. 4, pp. 439–455, 1975.

[10] D. M. Keenan, J. D. Veldhuis, and W. Sun, "A stochastic biomathematical model of the male reproductive hormone system," *SIAM Journal on Applied Mathematics*, vol. 61, no. 3, pp. 934–965, 2000.

[11] Y. Okada, Y. Fujii, J. P. Moore, and S. J. Winters, "Androgen receptors in gonadotrophs in pituitary cultures from adult male monkeys and rats," *Endocrinology*, vol. 144, no. 1, pp. 267–273, 2003.

[12] H. Taghvafard, A. Medvedev, A. Proskurnikov, and M. Cao, "Impulsive model of endocrine regulation with a local continuous feedback," *Math Biosci.*, pp. 128–135, Feb 2019.

[13] B. Goodwin, "Oscillatory behavior in enzymatic control processes," *Nature*, vol. 209, no. 5022, pp. 479–481, 1966.

[14] D. Gonze and W. Abou-Jaoudé, "The Goodwin model: behind the hill function," *PloS one*, vol. 8, no. 8, p. e69573, 2013.

[15] J. D. Murray, *Mathematical Biology, I: An Introduction (3rd ed.)*. Springer, New York, 2002.

[16] W. J. Heuett and H. Qian, "A stochastic model of oscillatory blood testosterone levels," *Bulletin of mathematical biology*, vol. 68, no. 6, pp. 1383–1399, 2006.

[17] A. Medvedev, A. V. Proskurnikov, and Z. T. Zhusubaliyev, "Mathematical modeling of endocrine regulation subject to circadian rhythm," *Annual Reviews in Control*, vol. 46, pp. 148–164, 2018.

[18] B.-Z. Liu and G. Deng, "An improved mathematical model of hormone secretion in the hypothalamo-pituitary-gonadal axis in man," *J. Theor. Biol.*, vol. 150, no. 1, pp. 51–58, 1991.

[19] D. Greenhalgh and Q. J. Khan, "A delay differential equation mathematical model for the control of the hormonal system of the hypothalamus, the pituitary and the testis in man," *Nonlinear Analysis: Theory, Methods & Applications*, vol. 71, no. 12, pp. e925–e935, 2009.

[20] N. Bairagi, S. Chatterjee, and J. Chattopadhyay, "Variability in the secretion of corticotropin-releasing hormone, adrenocorticotropic hormone and cortisol and understandability of the hypothalamic-pituitary-adrenal axis dynamics—a mathematical study based on clinical evidence," *Mathematical medicine and biology: a journal of the IMA*, vol. 25, no. 1, pp. 37–63, 2008.

[21] F. Vinther, M. Andersen, and J. T. Ottesen, "The minimal model of the hypothalamic–pituitary–adrenal axis," *Journal of mathematical biology*, vol. 63, no. 4, pp. 663–690, 2011.

[22] K. Sriram, M. Rodriguez-Fernandez, and F. Doyle III, "Modeling cortisol dynamics in the neuro-endocrine axis distinguishes normal, depression, and post-traumatic stress disorder (PTSD) in humans," *PLoS Computational Biology*, vol. 8, no. 2, p. e1002379, 2012.

[23] T. Tanutpanit, P. Pongsumpun, and I. Tang, "A model for the testosterone regulation taking into account the presence of two types of testosterone hormones," *Journal of Biological Systems*, vol. 23, no. 02, pp. 259–273, 2015.

[24] H. Taghvafard, A. V. Proskurnikov, and M. Cao, "Stability properties of the Goodwin-Smith oscillator model with additional feedback," *IFAC-PapersOnLine*, vol. 49, no. 14, pp. 131–136, 2016.

[25] ——, "Local and global analysis of endocrine regulation as a non-cyclic feedback system," *Automatica*, vol. 91, pp. 191–196, 2018.

[26] J. Mallet-Paret and G. Sell, "The Poincaré–Bendixson theorem for monotone cyclic feedback systems with delay," *J. Diff. Equations*, vol. 125, no. 2, pp. 441–489, 1996.

[27] A. Medvedev, A. Churilov, and A. Shepeljavyi, "Mathematical models of testosterone regulation," *Stochastic optimization in informatics*, vol. 2, pp. 147–158, 2006.

[28] A. Churilov, A. Medvedev, and A. Shepeljavyi, "Mathematical model of non-basal testosterone regulation in the male by pulse modulated feedback," *Automatica*, vol. 45, no. 1, pp. 78–85, 2009.

[29] Z. T. Zhusubaliyev, A. Churilov, and A. Medvedev, "Bifurcation phenomena in an impulsive model of non-basal testosterone regulation," *Chaos*, vol. 22, no. 1, pp. 013 121–1—013 121–11, 2012.

[30] P. Mattsson and A. Medvedev, "Modeling of testosterone regulation by pulse-modulated feedback," in *Advances in Experimental Medicine and Biology: Signal and Image Analysis for Biomedical and Life Sciences*. Springer, 2015, vol. 823, pp. 23–40.

[31] A. Churilov, A. Medvedev, and Z. T. Zhusubaliyev, "Impulsive goodwin oscillator with large delay: Periodic oscillations, bistability, and attractors," *Nonlinear Analysis: Hybrid Systems*, vol. 21, pp. 171–183, 2016.

[32] ——, "Discrete-time mapping for an impulsive Goodwin oscillator with three delays," *Int. J. Bifurcation and Chaos*, vol. 27, no. 12, p. 1750182, 2017.

[33] J. Veldhuis, D. Keenan, and S. Pincus, "Motivations and methods for analyzing pulsatile hormone secretion," *Endocrine Reviews*, vol. 29, no. 7, pp. 823–864, 2008.

[34] L. Krsmanović, S. Stojilković, F. Merelli, S. M. Dufour, M. A. Virmani, and K. J. Catt, "Calcium signaling and episodic secretion of gonadotropin-releasing hormone in hypothalamic neurons." *Proceedings of the National Academy of Sciences*, vol. 89, no. 18, pp. 8462–8466, 1992.

[35] P. Mattsson and A. Medvedev, "Estimation of input impulses by means of continuous finite memory observers," in *2012 American Control Conference (ACC)*, 2012, pp. 6769–6774.

[36] ——, "State estimation in linear time-invariant systems with unknown impulsive inputs," in *ECC 2013, July 17-19, Zürich, Switzerland*. IEEE, 2013, pp. 1675–1680.

[37] C. R. Fox, L. S. Farhy, W. S. Evans, and M. L. Johnson, "Measuring the coupling of hormone concentration time series using polynomial transfer functions," *Methods in enzymology*, vol. 384, pp. 82–94, 2004.

[38] J. D. Veldhuis, "Recent insights into neuroendocrine mechanisms of aging of the human male hypotalamic-pituitary-gonadal axis," *Journal of Andrology*, vol. 20, no. 1, pp. 1–18, 1999.

[39] J. P. Butler, D. I. Spratt, L. S. O'Dea, and J. W. F. Crowley, "Interpulse interval sequence of LH in normal men essentially constitutes a renewal process," *American Journal of Physiology-Endocrinology and Metabolism*, vol. 250, no. 3, pp. E338–E340, 1986.

[40] W. P. M. H. Heemels, K. H. Johansson, and P. Tabuada, "An introduction to event-triggered and self-triggered control," in *2012 IEEE 51st IEEE Conference on Decision and Control (CDC)*, 2012, pp. 3270–3285.

[41] U. Feudel, "Complex dynamics in multistable systems," *Int. J. Bifurcation and Chaos*, vol. 18, pp. 1607 – 1626, 2008.

[42] U. Feudel, A. Pisarchik, and K. Showalter, "Multistability and tipping: From mathematics and physics to climate and brain- Minireview and preface to the focus issue," *Chaos*, vol. 28, p. 033501, 2018.

[43] V. Avrutin, L. Gardini, M. Schanz, and I. Sushko, "Bifurcations of chaotic attractors in one-dimensional maps," *Int. J. Bifurcation and Chaos*, vol. 24, p. 1440012, 2014.

[44] G. C., O. E., and Y. J. A., "Chaotic attractors in crisis," *Phys. Rev. Lett.*, vol. 48, pp. 1507–1510, 1982.

[45] ——, "Crisis: Sudden changes in chaotic attractors and transient chaos," *Physica D*, vol. 7, pp. 181–200, 1983.

[46] Z. T. Zhusubaliyev, V. Avrutin, and F. Bastian, "Transformations of closed invariant curves and closed-invariant-curve-like chaotic attractors in piecewise smooth systems," *Int. J. Bifurcation and Chaos*, vol. 31, p. 2130009, 2021.